

OPTIQUE ET INTERFÉROMÉTRIE ATOMIQUES  
ATOM OPTICS AND INTERFEROMETRY

# Some theoretical and experimental aspects of three-grating Mach–Zehnder atom interferometers

R. DELHUILLE, C. CHAMPENOIS, M. BÜCHNER, L. JOZEFOWSKI, Th. LAHAYE,  
R. MATHEVET, A. MIFFRE, C. RIZZO, C. ROBILLIARD, G. TRÉNEC, J. VIGUÉ

Laboratoire collisions agrégats réactivité – IRSAMC, Université Paul-Sabatier and CNRS UMR 5589,  
118, route de Narbonne, 31062 Toulouse cedex, France  
E-mail: jacques@yosemite.ups-tlse.fr

(Reçu le 1<sup>er</sup> janvier 2001, accepté le 26 mars 2001)

## Abstract.

In this contribution, we present some recent theoretical results concerning the fringe contrast in Mach–Zehnder atom interferometers and the use of Bloch states to describe atomic diffraction. We also describe the observation of diffraction of lithium at thermal energy by a quasi-resonant laser standing wave. © 2001 Académie des sciences/Éditions scientifiques et médicales Elsevier SAS

cold atoms / interferometer / Bloch states / lithium / standing wave

## *Aspects théoriques et expérimentaux des interféromètres atomiques de Mach–Zehnder à trois réseaux*

## Résumé.

Dans cet article, nous décrivons nos résultats théoriques récents concernant le contraste des franges dans les interféromètres atomiques de Mach–Zehnder à trois réseaux et l'usage des états de Bloch pour décrire la diffraction d'atomes. Nous présentons aussi nos premiers signaux de diffraction d'un jet thermique de lithium par une onde stationnaire laser quasi-résonnante. © 2001 Académie des sciences/Éditions scientifiques et médicales Elsevier SAS

atomes froids / interféromètre / états de Bloch / lithium / onde stationnaire

## 1. Introduction

The first two parts of this contribution present a discussion of two questions concerning Mach–Zehnder atom interferometers: the fringe contrast, which presents a nontrivial dependence with the position of the detector, and the diffraction process. We show, in particular, that the use of Bloch states to describe the atom propagation inside the diffraction gratings largely simplifies the problem. The last part describes our first observation of diffraction of lithium atom at thermal energy by a quasi-resonant laser standing wave, an important step in the construction of our atom interferometer.

## 2. Fringe contrast in three grating Mach–Zehnder interferometers

We want to understand the fringe contrast in such interferometers. We start this study by developing a very simple model where the waves inside the interferometer are described by plane waves, but we are

Note présentée par Guy LAVAL.

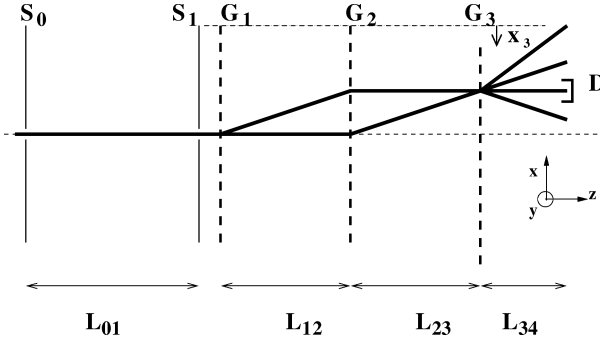


**Figure 1.** Schematic drawing of 3-grating Mach-Zehnder interferometers. Two collimating slits  $S_0$  (width  $e_0$ ) and  $S_1$  (width  $e_1$ ) define the incident beam which then goes through three gratings  $G_1$ ,  $G_2$  and  $G_3$ . Between the extreme gratings  $G_1$  and  $G_3$ , we have represented only two paths corresponding to the diffraction orders  $p_1 = +1$ ,  $p_2 = -1$  for the upper path,  $p_1 = 0$ ,  $p_2 = +1$  for the lower path, but we have represented various exits beams corresponding to different  $p_3$  values, some of these beams do not exist when the interferometer uses Bragg diffraction (in this case, the incidence angle of the beams on the gratings must be modified). The detector noted D collects the beams diffracted by the third grating.

well aware of the fact that diffraction must be taken into account in a complete analysis of this type of interferometer [1]. *Figure 1* represents schematically the interferometer and the interfering paths. Each of the three gratings  $G_j$  ( $j = 1-3$ ) is described by a wavevector  $\mathbf{k}_{gj}$  belonging to the grating plane and perpendicular to the grating lines. In the limit where  $|\mathbf{k}_{gj}| \ll |\mathbf{k}_a|$  and  $\mathbf{k}_{gj} \cdot \mathbf{k}_a \approx 0$ , where  $\mathbf{k}_a$  is the atomic wavevector, the diffracted wave corresponding to an incident plane wave  $\exp(i\mathbf{k}_a \cdot \mathbf{r})$  is given by:

$$\Psi_{p_j}(\mathbf{r}) = \alpha_j(p_j) \exp[i(\mathbf{k}_a \cdot \mathbf{r} + p_j \mathbf{k}_{gj} \cdot (\mathbf{r} - \mathbf{r}_j))] \quad (1)$$

where  $p_j$  is the diffraction order and  $\alpha_j(p_j)$  is the diffraction amplitude corresponding to this diffraction order. Finally,  $\mathbf{r}_j$  refers to the origin of the grating  $G_j$  which can be taken on anyone of the grating lines. The two interfering paths which are represented in *figure 1* corresponds to the diffraction orders  $p_1, p_2, p_3$  equal to  $+1, -1, 0$  for the upper path and to  $0, +1, -1$  for the lower path. The corresponding waves after the interferometer are given by:

$$\Psi_{\text{upper}}(\mathbf{r}) = \alpha_1(+1)\alpha_2(-1)\alpha_3(0) \exp[i(\mathbf{k}_a \cdot \mathbf{r} + \mathbf{k}_{g1} \cdot (\mathbf{r} - \mathbf{r}_1) - \mathbf{k}_{g2} \cdot (\mathbf{r} - \mathbf{r}_2))] \quad (2)$$

$$\Psi_{\text{lower}}(\mathbf{r}) = \alpha_1(0)\alpha_2(+1)\alpha_3(-1) \exp[i(\mathbf{k}_a \cdot \mathbf{r} + \mathbf{k}_{g2} \cdot (\mathbf{r} - \mathbf{r}_2) - \mathbf{k}_{g3} \cdot (\mathbf{r} - \mathbf{r}_3))] \quad (3)$$

We thus get the intensity  $I(\mathbf{r})$  of the atomic wave arriving at the point  $\mathbf{r}$  of the detector:

$$I(\mathbf{r}) \propto |\Psi_{\text{upper}}(\mathbf{r}) + \Psi_{\text{lower}}(\mathbf{r})|^2 \quad (4)$$

We will assume that the interferometer is symmetrical in the sense that the gratings  $G_1$  and  $G_3$  are identical. This insures that the amplitudes  $\alpha_1(+1)\alpha_2(-1)\alpha_3(0)$  and  $\alpha_1(0)\alpha_2(+1)\alpha_3(-1)$  associated to the two paths have the same modulus and for simplicity we assume that they have the same phase. Then, the intensity  $I$  is given by:

$$I \propto [1 + \cos(\Phi(\mathbf{r}) - \Phi_0)] \quad (5)$$

where  $\Phi(\mathbf{r}) = (\mathbf{k}_{g1} + \mathbf{k}_{g3} - 2\mathbf{k}_{g2}) \cdot \mathbf{r}$  and  $\Phi_0 = \mathbf{k}_{g1} \cdot \mathbf{r}_1 + \mathbf{k}_{g3} \cdot \mathbf{r}_3 - 2\mathbf{k}_{g2} \cdot \mathbf{r}_2$ . If the two interfering waves have not equal wavevectors, interference fringes appear in the detector plane. Integration over the surface of the detector will wash out any interference effect, resulting in a weak contrast. A good alignment of the three gratings is obtained when  $\Phi(\mathbf{r})$  does not depend on  $\mathbf{r}$ , which implies:

$$\mathbf{k}_{g1} + \mathbf{k}_{g3} = 2\mathbf{k}_{g2} \quad (6)$$

As expected, this condition simply means that the two interfering beams have equal wavevectors. Then, the interferometer signal given by  $I \propto [1 + \cos(\Phi_0)]$  depends only on the value of  $\Phi_0$ , i.e. of the relative position of the origins  $r_i$  of the three gratings (this is due to the fact that no phase object has been introduced in the two interfering paths). The presence of  $\Phi_0$  in the interferometer signal is used to observe fringes by displacing one of the gratings in its plane in a controlled manner. The fringe contrast is then equal to 1. This term also reflects the response of the signal to vibrations: the sensitivity to grating displacements is large. Nevertheless, the scale of the displacement needed to sweep one fringe is just the grating period, not the atomic wavelength. This is easy to explain in the case of amplitude gratings, following an argument developed by D. Pritchard and coworkers [2]: the two coherent atomic beams (propagating along the lower and upper paths shown in *figure 1*), when they recombine on the third grating, form a stationary atomic wave which has exactly the grating period. The observation of fringes is therefore explained by a Moiré filtering effect of the stationary atomic wave by the third grating.

This discussion explains why a motion of the third grating permits the observation of fringes and, at the same time, the alignment condition (6). It also explains why the contrast is less than 1, if the detector is placed immediately after the third grating  $G_3$ : in this case, the detector intercepts many different beams exiting from the interferometer and the contrast can be calculated as the product of the contrast  $C_0$  of the atomic standing wave formed in the plane of  $G_3$  by a contrast  $C_M$  due to the Moiré filtering process.

The Moiré filtering effect does not exist when the gratings are phase gratings: with phase gratings, the contrast vanishes if the detector placed immediately after the third grating  $G_3$  and the contrast increases when the various beams produced by diffraction by this grating separate (see *figure 1*). These beams correspond to the interference of the upper paths  $+1, -1, p_3$  and of the lower paths  $0, +1, p_3 - 1$  for various  $p_3$  values. As these paths carry contrast of opposite signs (i.e. the intensity is maximum for values of the phase  $\Phi_0$  differing by  $\pi$ ), the total contrast is reduced because it results from the sum of the contributions of the different paths reaching the detector.

This simple model is too rough to fully describe the propagation of the atomic waves inside the interferometer and we have developed a calculation of the atomic intensity in the detector plane. This calculation is based on the scalar diffraction theory. The diffraction due to the collimation slit occurs in the Fresnel regime and this feature makes the calculations much more complex. A first calculation of this type was developed in 1992 by Q. Turchette, D. Pritchard and D. Keith [3], with the multidimensional integrals calculated by numerical techniques. Using change of variables and analytic results, we have been able to reduce by a large factor the amount of numerical computation [1]. We have thus been able to calculate the fringe contrast in many cases, including the case of a slightly misaligned apparatus. In our published work [1], we have considered either amplitude gratings like the ones used in the experiments of D. Pritchard and coworkers, or phase gratings using laser diffraction operating in the Raman–Nath regime. We will not reproduce these results here, because, as demonstrated by the experiments of Siu Au Lee and coworkers [4, 5], we feel now that the practical diffraction regime for an interferometer using laser diffraction is the Bragg regime. So, we have calculated the fringe contrast as a function of the distance  $L_{34}$  from third grating to detector for a perfect interferometer in the Bragg regime and this result is shown in *figure 2* (for simplicity, the amplitudes are taken at their optimum values:  $1/\sqrt{2}$  for the gratings  $G_1$  and  $G_3$  which play the role of beam-splitters and 1 for  $G_2$  which play the role of mirrors, neglecting the dispersion of these amplitudes due to angular and velocity distribution of the incident atomic beam).

### 3. Atom diffraction by laser: theoretical analysis

We consider here the simplest case of atomic diffraction by a quasi-resonant laser standing wave. If the laser detuning is sufficient, no real excitation will occur and in the dressed-atom picture [6], one shows that the only effect of the laser standing wave is to create a light shift potential  $V(x, z)$ :

$$V(x, z) = V_0(z) \cos^2(k_L x) = \frac{V_0(z)}{4} [2 + \exp(+ik_g x) + \exp(-ik_g x)] \quad (7)$$

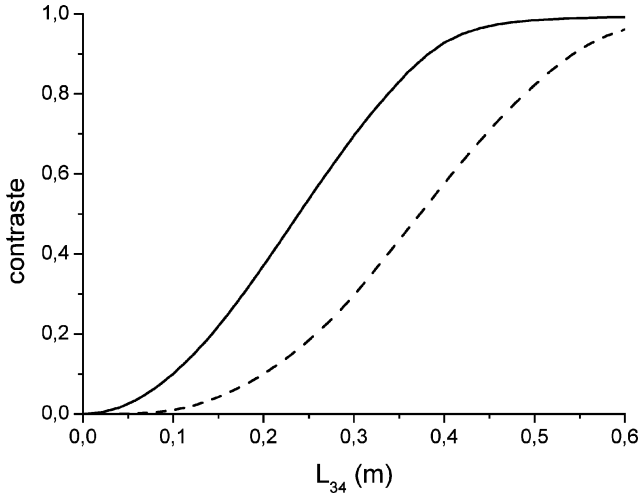


**Figure 2.** Contrast of the fringe pattern as a function of the distance from grating  $G_3$  to the detector. The gratings are phase gratings using Bragg diffraction. The contrast vanishes when the detector is located close to  $G_3$  and reaches the value 1 when the various beams separate. Two calculations have been made corresponding to collimating slit widths  $e_0 = e_1 = 20 \mu\text{m}$  and a detector slit width  $e_D = 50 \mu\text{m}$  (full line) or  $100 \mu\text{m}$  (dashed line).

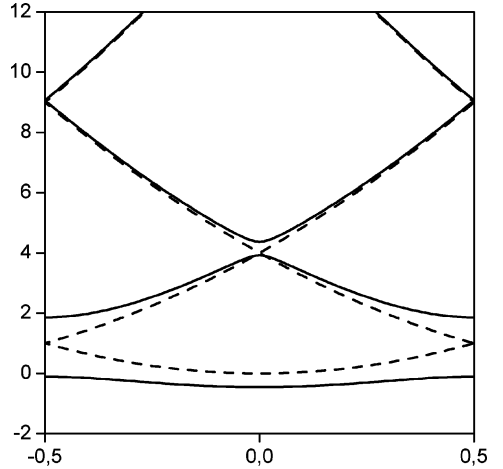


**Figure 3.** Plots of the energies  $\varepsilon$  of the lowest Bloch states belonging to the first Brillouin zone versus the quasimomentum  $k$  measured in  $k_g$  unit. The energy unit is  $\hbar\omega_{\text{rec}}$  and the energy diagram has been plotted for two values of the potential strength parameter  $q = V_0/4\hbar\omega_{\text{rec}}$ : solid line  $q = 1$ , dashed line,  $q = 0$ . A global energy shift equal to  $V_0/2$  has been omitted.

We have assumed that the laser beams propagate along the  $\pm x$ -direction and their width along the  $z$ -direction is equal to  $D$ . The grating wavevector  $k_g$  is related to the laser wavevector  $k_L$  by  $k_g = 2k_L$ . If the laser beams are not limited in the  $y$  direction, the motion in this direction is free and it can be completely forgotten in the present discussion. To treat the diffraction process, the  $(x, z)$  plane is divided in three regions (before, in and after the grating) and the atomic wavefunction is written explicitly in these three regions and linked by continuity equations [7]. In region 1, which is the vacuum for  $z \leq 0$ , the atomic propagation is described by an incident plane wave:

$$|\Psi_1\rangle = |k_{x1}\rangle|k_{z1}\rangle \tag{8}$$

Region 2 is the grating extending from  $z = 0$  to  $z = D$  and we assume  $V_0(z)$  to be constant and equal to  $V_0$ . In this region, the motion in the  $z$ -direction is free and described by plane waves while the motion in the  $x$ -direction is described by atomic Bloch states. The Bloch states and their energies are noted  $|k, p_2\rangle$  and  $\varepsilon(k, p_2)$  respectively (see figure 3). Here,  $k$  is the quasi-momentum chosen in the first Brillouin zone and  $p_2$  is an integer labeling the energy bands. The wavefunction is given by:

$$|\Psi_2\rangle = \sum_{k, p_2} b_{p_2}(k) |k, p_2\rangle |k_{z2}(k, p_2)\rangle \tag{9}$$

Finally, region 3 is the vacuum for  $z \geq D$ , where the atomic wave is described by a sum of plane waves corresponding to the various diffraction orders:

$$|\Psi_3\rangle = \sum_{p_3} c_{p_3} |k_{x3}(p_3)\rangle |k_{z3}(p_3)\rangle \tag{10}$$

We use the continuity of the wavefunction and its normal derivative in the  $z = 0$  and  $z = D$  planes. In order to simplify the calculations, we assume that the atom total energy given by the initial kinetic energy,  $E = \hbar^2 k_1^2 / 2m$ , is considerably larger than  $V_0$ . It is a good approximation to neglect the reflected atomic waves and then the two continuity equations are equivalent. The plane waves contributing to the transmitted wave (10) verify  $k_{x3}(p_3) = k_{x1} + p_3 k_g$ , where  $p_3$  is the diffraction order and the diffraction amplitude  $c_{p_3}$  is given by:

$$c_{p_3} = \sum_{p_2} \langle k_{x3}(p_3) | k, p_2 \rangle \langle k, p_2 | k_{x1} \rangle \exp[i(k_{z2}(k, p_2) - k_{z3}(p_3))D] \quad (11)$$

The  $z$ -components of the wavevectors in regions 2 and 3 can be calculated using energy conservation:

$$\frac{\hbar^2(k_{x1}^2 + k_{z1}^2)}{2m} = \varepsilon(k, p_2) + \frac{\hbar^2 k_{z2}(k, p_2)^2}{2m} = \frac{\hbar^2(k_{x3}^2 + k_{z3}^2)}{2m} \quad (12)$$

As long as  $q$  (defined below) and  $k_{x1}/k_g$  are not too large, the important contributions in equation (11) come from small values of  $p_2$  for which the dependence of  $k_{z2}(k, p_2)$  with  $p_2$  is weak, but this dependence with  $p_2$  of the accumulated phases nevertheless creates the diffraction effect. If the propagation phases appearing in equation (11) were independent of  $p_2$ , a sum rule would appear and only one plane wave would be transmitted in medium 3, corresponding to the zeroth diffraction order. We think that this formalism opens a new viewpoint on the diffraction process, with improved physical insight, as the associated calculations remain very simple. We have also shown [7] that we can relax the simplifying hypothesis of discontinuous media in the planes  $z = 0$  and  $z = D$  and thus treat more realistic cases.

To go further in this discussion, we must consider various diffraction regimes. Following the discussion presented by C. Keller et al. [8], the problem involves three parameters: the potential strength  $V_0$ , the atom recoil energy  $\hbar\omega_{\text{rec}} = \hbar^2 k_L^2 / 2m = \hbar^2 k_g^2 / 8m$  and the interaction time  $t_{\text{int}}$  of the atom with the grating. For an incidence near normal incidence, the velocity  $v_z$  is closely approximated by  $v_z \approx \hbar k_1 / m$  and the interaction time is given by  $t_{\text{int}} = D / v_z \approx mD / (\hbar k_1)$ . With these three parameters, we build two dimensionless parameters, namely a reduced potential strength  $q$  given by:

$$q = V_0 / (4\hbar\omega_{\text{rec}}) \quad (13)$$

and a reduced interaction time  $\tau_{\text{int}}$  given by:

$$\tau_{\text{int}} = \omega_{\text{rec}} t_{\text{int}} \quad (14)$$

As an example, we discuss briefly two limiting cases:

- The Raman–Nath regime corresponds to the limiting case  $q \rightarrow \infty$  and  $\tau_{\text{int}} \rightarrow 0$ , while keeping a finite value of the phase  $\gamma = 2q\tau_{\text{int}}$ . Then, the probability of diffraction of order  $p_3$  is given by a classical formula:

$$P_{p_3} = |J_{p_3}(\gamma)|^2 \quad (15)$$

It is easy to show that the validity range of this approximation is  $\tau_{\text{int}} < 1/4\sqrt{q}$  and our technique [7] permits very easily to test this validity range by working with different values of the potential strength parameter  $q$ .

- The first order Bragg diffraction regime corresponds to an incidence such that  $k_{x1} = k_g/2 = k_L$ . Then, when the potential is weak ( $q \lesssim 1$ ), the free wave arriving from region 1 is projected on two Bloch states. When the potential term  $V_0$  vanishes, these two states are exactly degenerate and they correspond to the plane waves  $|k_x = \pm k_g/2\rangle$ . The problem is then equivalent to a Rabi oscillation between these two plane waves. The diffraction efficiency reaches 1 when the interaction time  $\tau_{\text{int}}$  is such that the phase

$\gamma = 2q\tau_{\text{int}}$  is equal to  $\pi$ . It is remarkable that the Bragg diffraction regime is observed when there is an avoided crossing in the energy diagram of Bloch states. This is true not only for first order Bragg diffraction, but also for all other orders: even and odd diffraction orders corresponds to avoided crossings respectively in the center or on the border of the first Brillouin zone. In all cases, if the  $q$  parameter is not too large, the problem reduces to a two level problem with a solution of the Rabi oscillation type.

#### 4. Atom diffraction by laser: experiment with lithium

We report here the observation of diffraction of a thermal atomic beam of lithium by a laser standing wave. After a brief description of the main characteristics of the experimental setup, we will present our observation of Bragg diffraction.

##### 4.1. Experimental setup

The lithium atomic beam is produced by supersonic expansion of lithium vapor seeded in argon. The temperature of the backpart of the oven is 870 K corresponding to a lithium pressure close to 0.1 mbar while the nozzle is slightly overheated near  $T_0 = 920$  K to prevent clogging. The argon pressure is 0.3 bar and the nozzle diameter is 300  $\mu\text{m}$ . The calculated beam mean velocity  $u$  is  $\sqrt{5k_B T_0/m_{\text{Ar}}} \approx 980$  m/s corresponding to a de Broglie wavelength  $\lambda_{\text{dB}} \approx 58$  pm.

The lithium beam encounters successively the following elements defined by their sizes and their distance  $z$  from the nozzle: a 1 mm diameter skimmer at  $z = 0.02$  m, two 45  $\mu\text{m}$  wide vertical collimating slits respectively at  $z = 0.4$  m and  $z = 1.2$  m, the laser standing wave at  $z = 1.3$  m, a movable vertical detection slit at  $z = 2.5$  m and a surface ionization detector made of a 760  $\mu\text{m}$  wide hot wire (a rhenium ribbon) at  $z = 2.9$  m. The lithium atoms are ionized with a large probability when they hit a rhenium hot ribbon and the ions are detected by a Channeltron followed by a fast counting electronics. The signals represent the number of detected ions as a function of the detection slit position.

The laser standing wave is produced by an argon ion pumped single frequency dye laser. A telescope made of two converging lens of long focal length is used to expand the beam, which then enters the vacuum chamber through an antireflection coated window and it is back reflected by a mirror under vacuum. The direction perpendicular to the mirror surface defines the standing wave and we have to orient carefully this mirror to reach the Bragg condition.

##### 4.2. Results

In a first time, we have recorded the profile of the atomic beam, in the absence of laser. This experiment is useful to verify the good alignment of the various collimating elements and, using this signal, we can optimize this alignment and the intensity of the beam. The transverse profile is in good agreement with our simulations. In the best conditions, we obtained count rates of the order of  $3 \cdot 10^4$  s $^{-1}$  with a 100  $\mu\text{m}$  wide detection slit. The experimental data presented here were recorded with a 50  $\mu\text{m}$  wide detection slit to achieve a better separation of the diffraction peaks.

We then introduce the laser beam and we tune the orientation of the mirror in order to observe diffraction in the first order. Once this alignment obtained, we scan the position of the detection slit to observe the various diffraction orders. We have collected several curves corresponding to various laser powers, various values of the frequency detuning (about 1–3 GHz to the blue of the  $^2S_{1/2}$ – $^2P_{3/2}$  line) and various waist radius. *Figure 4* presents such an experimental curve: the presence of the first diffraction order on only one side of the direct beam is a clear signature of Bragg diffraction. The diffraction peak splitting is in good agreement with the calculated value of the diffraction angle  $\theta = 2\lambda_{\text{dB}}/\lambda_{\text{L}} \approx 170$   $\mu\text{rad}$ .

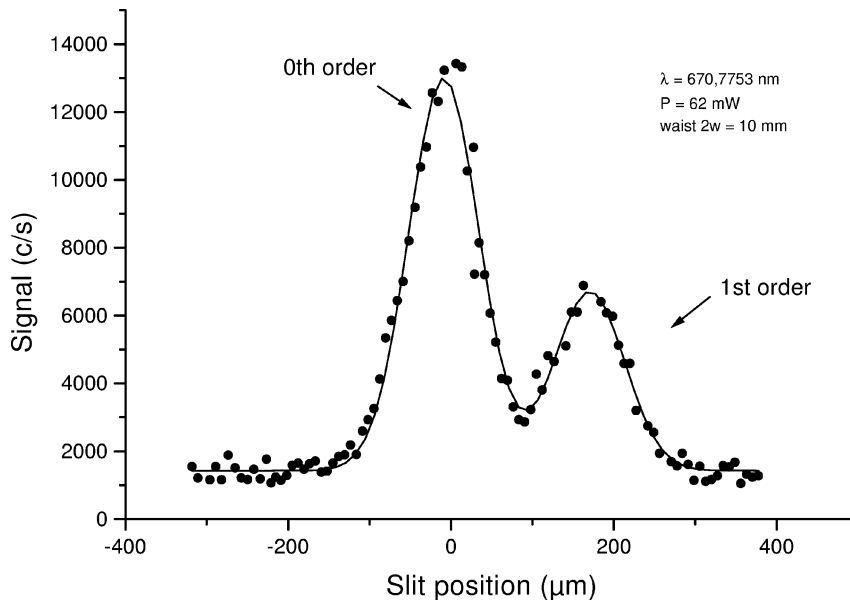


**Figure 4.** Number of atoms detected per second as a function of the detector slit transverse position in  $\mu\text{m}$ . Two peaks are present, corresponding to the diffraction order 0 and +1. The complete absence of the peak corresponding to the order  $-1$  is a clear proof that the diffraction operates in the Bragg regime.

## 5. Conclusion

In this talk, we have described three steps concerning the construction of an atom interferometer. We have developed a complete model of the propagation of atomic waves in Mach–Zehnder interferometers. This model which complements the calculation done by D. Pritchard and coworkers will be very helpful to optimize the fringe contrast in our apparatus. We have also developed a unified formalism using atomic Bloch states to describe atom diffraction by a quasi-resonant laser standing wave. This formalism provides a very good insight in the diffraction process and it is very useful to choose the parameters defining the laser standing waves. Moreover, Bragg diffraction is classically reduced to a two level problem with a Rabi-type oscillation solution and, in our formalism, we can easily explore the limits of this approximation by extending the Bloch basis set. Finally, we have presented here our first observations of laser diffraction of a lithium atomic beam in our experiment, thus proving that most of the necessary components of an atom interferometer are already working.

## References

- [1] Champenois C., Büchner M., Vigué J., *Eur. Phys. J. D* 5 (1999) 363.
- [2] Schmiedmayer J., Chapman M.S., Ekstrom C.R., Hammond T.D., Kokorowski D.A., Lenef A., Rubinstein R.A., Smith E.T., Pritchard D.E., in: P.R. Berman (Ed.), *Atom Interferometry*, Academic Press, 1997, p. 1.
- [3] Turchette Q., Pritchard D., Keith D., *J. Opt. Soc. Amer. A* 9 (1992) 1601.
- [4] Giltner D.M., McGowan R.W., Lee Siu Au, *Phys. Rev. A* 52 (1995) 3966.
- [5] Giltner D.M., McGowan R.W., Lee Siu Au, *Phys. Rev. Lett.* 75 (1995) 2638.
- [6] Cohen-Tannoudji C., Dupont-Roc J., Grynberg G., *Atom–Photon Interactions*, Wiley, 1998.
- [7] Champenois C., Büchner M., Delhuille R., Mathevet R., Robilliard C., Rizzo C., Vigué J., *Eur. Phys. J. D* 13 (2000) 271.
- [8] Keller C., Schmiedmayer J., Zeilinger A., Nonn T., Dürr S., Rempe G., *Appl. Phys. B* 69 (1999) 303.